

# The *Mycobacterium abscessus* cytochrome bcc:aa3 oxidase structure paves the way for an agent targeting subunit QcrB

Corresponding Author: Professor Gerhard Grüber

This file contains all reviewer reports in order by version, followed by all author rebuttals in order by version.

Version 0:

Reviewer comments:

Reviewer #1

(Remarks to the Author)

This manuscript by Mathiyazakan et al., describes the structures of cytochrome bcc:aa3 oxidase super complex from *Mycobacterium abscessus*, an opportunistic mycobacterium, which is less sensitive to some drugs designed for *Mycobacterium tuberculosis* for example bedaquiline. The enzymes in electron transport chain and the ATP synthase of the *Mycobacterium* have been targets for drug design (example bedaquiline). With the advent of cryoEM as structural biology technique, the enzymes and the super complexes of the ETC from *Mycobacteria* and related bacteria have been determined illuminating their architecture and mode of drug binding providing way for better design of small molecules. Here, the authors purify and determine the structure of the super complex containing bcc and aa3 type oxidase from *M. abscessus* revealing conserved and salient features. Analysis of the binding pocket in one subunit, where the drug binds and that inhibits *M. tuberculosis* reveal differences and this was exploited to design a new drug, which showed high potency against *M. abscessus* and related species. The determined structure with the drug showed the mode of binding, explaining how small changes in the residues (here Glu to Asp and Ala to Leu) can make a huge difference. The major strength of the manuscript is the explanation of the binding mode of inhibitor and mutagenesis to show how the activity is affected. However, the description and writing of the manuscript needs to be greatly improved and the figures, which require clarity. Please find below comments and suggestions that might help to improve the manuscript.

1) An important thing that is not clear to me from the materials and methods, how the water molecules were modelled. The reported resolutions of the two maps are ~2.3 and 2.9 Å but the same number of modelled water molecules (74 – from the PDB validation files) is given for both models. The modelled water molecules are shown in figures 4 and 8, and described in the sections of proton pathways and H<sup>+</sup> translocation. How were they modelled? Were they derived from previous models of other structures? One would expect the map with inhibitor and higher resolution should have more water molecules (in theory at least). Some description of this will be useful and to be added in the method.

2) The method section describing the cryoEM imaging data collection and processing is condensed and has not much details (and also not in the supplementary figure describing the workflow). Example, lines 403 and 413 says data processing was performed with cryosparc. Here or in the workflow, how the movies were filtered (criteria for curation), how many models/classes were requested for ab-initio, 3D classification can be described. Also, in the references (34,35) – one for cryosparc and Relion is given (I presume for global refinement). For a casual reader, reference 35 – Zivanov et al indicates that relion was used but this is not case here but for aberration correction. A reference for non-uniform refinement should also be added (Punjani et al 2020).

3) Line 403 and 414 says 'structure refinement was done using COOT and Phenix software' should rather be 'Model building and refinement was performed using Coot and Phenix'. This should be expanded (as described in point 1, how was the initial model obtained – denovo or previous PDBs), modelling of ligands etc., If this is included here, then the section heading should read 'CryoEM data collection, processing, model building and refinement' instead of 'CryoEM data collection, processing'. Also, reference number 36 is not apt here and more appropriate references are Emsley et al 2004 (Acta D) and Casanál et al 2020.

4) In supplementary figure 1 and 6, the FSC curves showing the map vs model should be included and resolution reported at 0.5.

5) Figure 1 is not referred in the text and the relevance of having in the manuscript is not clear. I don't think it adds any value. If in case this needs to be retained then best be as a supplementary figure.

6) Line 93 – is the native PAGE mentioned a 'blue-native PAGE'? If yes, reference needs to be added and described in the methods.

7) Line 99-100 – 6,845 movies yielded 249,718 particles. This sentence needs rephrasing as the original particles after picking is 956580, but of the 6485, 1305 movies were removed (as per Supp Fig 1).

8) For supplementary figures 2-4, I have few suggestions. In Supp figure 2, the cartoon representation be replaced with stick representation so that the backbone tracing can be easily followed. In supp figure 3, in my opinion, the interacting/surrounding residues of the ligands within the density should also be shown, in particular for the metal ligands as they look odd by themselves. In supp figure 4, can the backbone be changed to another color instead of gray as the map is also in the same color. In all these figures, the contour level used for the maps be given in the legend and I presume made using Pymol. If yes, then the reference to be added.

9) In the main figure 3, I feel that it is important to have the cryoEM map as the modelling is based on the map (and the experimental data). So, a panel with the map colored as in 3A will be very helpful. In panel A, density for SOD is shown – how was this figure made i.e., to show only SOD density and it is mentioned (line 121-123) seen at low resolution at 7.5 Å (if it was made with Chimera, then the reference needs to be included). Not clear if it is visible only lower threshold as it is smeared out due to sharpening. In this regard, did the classification or ab-initio give any hint of populations with and without SOD. Can this be elaborated perhaps in the methods. In panel 3A, can the assembly factor be labelled (PRSAF and LpqE)? Bit difficult to spot them as the colors are similar (but possible when panel B is referred).

10) The sentence in line 123 – 'The catalytically active CtaC and CtaD contain their cofactors within the cyt-aa3 domain are CtaC and CtaD' – doesn't make sense.

11) I am not sure if the section electron and proton translocation pathway needs to be in this detail. I guess these are not new structures i.e., high similarity between the structures of Mab with Msmeg/Mtb and related species. Will it help to focus only on key features.

12) Figure 4 is perhaps easily understood by experts in the field of structural bioenergetics but not by a non-expert. For instance, panel A can have surface representation of the protein and highlighting ligands and in the rest of the panels also the cartoon from the protein molecule dominates (make them thinner or change from cylinder to another form).

13) Line 137, I think the Fig. 3B should be 4B

14) In the section, residues responsible for Q203 inactivity .. there is description of residues and the cavity being smaller. But it would help to give some numbers by providing the volume/size of the cavity in different species (example as shown in panel 5B). This would help because in line 218, it is mentioned 'the reduction in the Mab cyt-bcc:aa3 cavity volume'.

15) In figure 5, the comparison (panel A) of 3 models has closely related colors – blue (Mtb, apo), green or cyan (Mtb +Q203) and purple (Mab), this makes it difficult to follow, can this be relooked.

16) In figure 7A, the structure of ND-011458 has a cyclobutane ring in position 1 (a square), is this correct? I thought the compound was synthesized to have only a methyl group from Q203 (I am not a chemist, so I might be wrong in this). In the supplementary figure showing the synthesis (and in validation file), the molecule doesn't have this.

17) Line 242, this refers to Fig 6E, should this be 7E?

18) In Supplementary figure 6, the panel A is not required (doesn't add much).

19) Figure 8 needs some rethink. It is important to show the density of the ligand (ND-011458) more clearly along with surrounding residues. In the current form, it is shown but not so good. I think panel D should come after panel A and then B/C. In panel B and C, secondary structures can be removed or made thin (like suggested for figure 4). In particular, panel C looks odd with a grey background.

20) Line 282, as revealed in figure 8A, CFZ reduced the MIC50? CFZ is not shown anywhere, should this refer to panel 8E?

21) Line 301, 'Guided by these insights, we discovered ND-011458 ..' I think more appropriate will be 'Guided by these insights, we designed ND-011458'. This is because a new drug has not been identified from a library or from scratch but merely restricting to only a methyl group from an existing compound guided by the structure. In this regard, a MSA of different species of Mycobacteria and other related bacteria focused only on the QcrB or the cavity region might add value.

22) In table 2B, the particle images/numbers need to be revised. When it says selected, it can be from any of the steps from picking to classification. May be an easy way is to use the initial particle numbers – after autopick and then clean up after 2D classification (before ab-initio) and then final number contributing to the map. Here, in the ND-011458 data, the numbers are different than in the work flow (supp figure 6), please check. The applied B-factor (Å<sup>2</sup>) should be with negative sign (as the map is sharpened). Global resolution is mentioned as 2.66 but the validation file has 2.85 Å. Tables 2A and 2B can be combined by removing the whole image processing section as this is mentioned in the methods.

23) In table 2C, the number of residues is the same for both the models. This is surprising as one of them has ligand (2 numbers). In the validation file, I notice that chain k/l in the apo model has 144 residues (46750 atoms as in the validation file) and, in the inhibitor, bound structure has 145 residues (46789 atoms in the validation file). Summing up the number of residues in the validation file gives a number of 5756 for the dimer, which is different from 5634 in the table. Please check. I would recommend the table to be expanded to include number of residues for proteins, ligands, water separately and the B-factors (after model refinement) for each of them. Alternatively, number of atoms (for proteins, ligands and water) can be mentioned instead of residues as done routinely in crystallographic structures.

24) In the PDB validation file of the apo structure (9WCX), there is one peculiar bond length outlier (among others) – chain X, Thr43, the N-CA is 2.52 Å, which is 1.1 Å longer than the ideal values. Please check this.

Other comments:

Line 237 – IC<sub>50</sub>, change 50 to subscript

Line 367 – should be '100 µg/ml 3x FLAG peptide'

Line 397 – I think this should K3 and not K2. If it is K2, then the exposure time has to be higher (not 2.83 s as mentioned in line 400).

Line 401/412 – it should be CTF estimation and not refinement. CTFFIND4 estimates the CTF from the images.

Line 410 – 0.5 to 1.5  $\mu\text{m}$  and not  $\mu\text{M}$

Line 460 – should read, 'In this assay, Laminin/poly-D-lysine ...'

Figure 2 panel A, there are 3 lanes labelled as -, + and Mab, two showing positive signal in Western blot. Are these two lanes with different concentration or volume? Or in other words, what are(+), Mabs. The lane numbers can be given in the bottom.

Figure 7, panel A, Design of Q203 analogues with modifications at position 1. Were there many more analogues made?

## Reviewer #2

### (Remarks to the Author)

Mathiyazakan et al. describe purification of the mycobacterial bcc-aa3 supercomplex from *Mycobacterium abscessus*, and two structures of this complex that they have solved by cryoEM single particle methods. Structures are available from *M. tuberculosis* and *M. smegmatis*, but *M. abscessus* is a pathogen in its own right and has different inhibitor sensitivity than *M. tuberculosis*, justifying the work.

Of four mutational differences near the active site, they determined by site-directed mutagenesis that two were important, and designed a new inhibitor based on the structure that should be more effective against *M. abscessus*. They prepared a tagged strain of the complex, purified it, and solved the structure of the native complex, one with menaquinone in the binding sites and the other with the new inhibitor in the Qo site. The work is sound and significant, but there are a number of errors in the manuscript that should be addressed.

Fig 1. On the left hand figure, showing the mitochondrial situation, the space below the membrane is labeled cytoplasm. This is OK if we ignore the outer mitochondrial membrane due to its permeability. But the space above should then be "mitochondrial matrix", not periplasm. To further confuse, the membrane is concave downward, suggesting that the cytoplasm is inside and the matrix or periplasm is outside.

On the other hand if we assume the labeling is for bacterial counterparts, with cytoplasm = matrix below and periplasm = inter-membrane space above, the orientation of the complexes is wrong, as cyt c and the P-side of the complexes should be in the inter-membrane/periplasmic space.

Fig 1 legend, line 549: ". . the dominant oxidase cyt-bo3 (cyan-green) resembles a CIII-CIV like assembly"  
insert the word "functionally", because structurally there is little similarity.

114-116: The description of subunit qcrC seems to be wrong- the trans-membrane helix is on the C-terminal end, not the N-term as implied

here. That is, "after" the periplasmic heme-binding domain, not before.

lines 142-144, 304: "low-spin, high-spin, heme". Is this supposed to be low, high potential heme?

Both B hemes are low spin, with bi-axial histidine coordination.

94 ". . . the presence of hemes a, b and c," -

There is a convention, (although maybe not official), of referring to heme with capital letters when just specifying the type of heme, i.e. the substance, rather than heme of a specific cytochrome. thus, "heme bL and heme bH are both B hemes, the complex contains two heme B molecules". I leave up to the authors' discretion.

line 315- protonatable QcrB residue s155 D311, R315, D304 and E272,  
E272 is in qcrC, according to figure 4. This should also be made clear here.

The oxygen consumption assay in Figure 2E is problematic and needs more explanation. It should be stated what is added at ~50 s. If I understand correctly, the enzyme was present from the start and reduced DMNQ was added at 50 s. The decrease in oxygen in the control could be due to dilution by the anaerobic DNQH2 solution, but only if the dilution is greater than 2-fold (volume of DNQH2 is not given). Otherwise there is concern that the reduction is due to residual BH4, H2 reacting at the platinum Clark electrode, or some rapidly auto-oxidizable substance reduced by BH4.

In the trace with enzyme, the decrease in O2 on adding DMNQH2 is greater, reaching nearly to zero, mostly within about 10 sec. The assumption would be that this is due to oxygen consumption by the complex. Using a lower concentration of enzyme might permit to resolve the enzyme activity from

the dilution effect and electrode kinetics. Or maybe I completely misunderstand the assay, due to lack of description.

It would be nice to have a third trace with enzyme plus inhibitor, and a fourth trace with enzyme + KCN or other inhibitor of the oxidase (is NQH2 reacting at Qo, or directly with the C hemes?). Finally, adding dithionite at the end would establish the zero O2 level.

However it is understood that the main focus of the paper is on structure not activity, so just providing a better explanation would be acceptable.

Line 135: "The distinct coulombic densities for MQH2 and menaquinone (MQ), at the Qo sites and Qi sites, respectively . . ." Can you really distinguish MQ from MQH2 at this resolution)? And, if the enzyme is active it should oxidize MQH2 at Qo and reduce MQ at Qi, giving the opposite of what you suggest. More likely both would be oxidized when applied to the grid, maybe reduced by the electron beam/radiation damage.

line 239 and 623- "ND-011458 was able to achieve the characteristic respiratory burst observed for Q203 in Mtb".  
Need to briefly explain why a respiratory inhibitor causes a respiratory burst. Is respiration going by an alternate oxidase with lower efficiency, thus needing more O2?

line 374, 376. "The oxidized UV spectra" - The shortest wavelength shown is 425 nm.

I did not have access to the structure coordinates files, which are on hold until publication. I would have liked to see if they found the cis-prolines at residues 138,257, and maybe 421 in qcrB. The validation reports from Protein Data Bank were made available, and did not raise any alarms. But then I am not very familiar with cryo-EM methods and validation.

The resolution is given as 2.6 Å. Which of the two structures is this for? Do they both have the same resolution?

Sup fig 1 legend: (B) "2D- classification in of picked particles in . . ." delete "in" or "of"

Edward Berry

Reviewer #3

(Remarks to the Author)

In the manuscript of Mathiyazakan et al, entitled 'The Mycobacterium abscessus cytochrome bcc:aa3 oxidase structure paves the way for a new agent targeting subunit QcrB' the authors present the cryo-EM structure of M. abscessus cytochrome bcc:aa3.

A comparison to the cytochrome bcc:aa3 structure of M. tuberculosis reveals that an alanine to leucine substitution and a glutamate to aspartate substitution from M. tuberculosis to M. abscessus prevents the binding of the well-known cytochrome bcc:aa3 inhibitor Q203 (also known as Telacebec). Inversion of these two residues (i.e. L314A and D311E) restores sensitivity of M. abscessus to Q203. They then show that a predicted steric clash between the leucine 314 and the ethyl group at the imidazol[1,2a]pyridine moiety of Q203 can be remediated by changing the ethyl group to the shorter methyl group. This modified variant of Q203, termed ND-011458, shows potent inhibition of the growth M. abscessus cells and oxygen consumption of the purified M. abscessus cytochrome bcc:aa3 complex. Finally, they show that their new inhibitor, ND-011458, acts synergistically with the antibiotic clofazimine.

Overall, the manuscript is well-written, and the figures are clear.

However, I have concerns about the novelty of the work. Currently, there are 15 mycobacterial cytochrome bcc:aa3 structures available in the protein data bank and 7 papers that describe these. There are no major differences between the new M. abscessus structure and previous structures that change the interpretation of catalytic cycle. Hence, the detailed description of this cycle presented on pages 5-8 (lines 105-182) is a repeat of earlier work (see doi: 10.1038/s41594-018-0160-3, 10.1126/science.aat8923, and 10.1038/s41467-024-49628-9.)

The observation that the modification of two residues in the inhibitor binding site or the deletion of one methyl group in the Q203 inhibitor restores sensitivity of M. abscessus to this class of compounds is nice, but not surprising.

In addition, the observation that this class of compounds synergizes with clofazimine is not new either, as this has been described before (see doi: 10.1128/aac.00318-25, 10.1016/j.biopha.2020.110782, 10.1128/AAC.01418-21, 10.1128/aac.00318-25, 10.1038/ncomms12393)

Finally, there are more than twenty Q203-like compounds that have been described to date. Currently, the most advanced of these, Q203, appears to be stalled after the Phase-2 clinical trials. None of the other Q203-like inhibitors has entered the clinical trial stage. This shows that the progress from an initial inhibitor such as ND-011458 to late-stage lead compound such as Q203 is extremely challenging. Thus, the addition of another compound to the growing list of cytochrome bcc:aa3 inhibitors is unlikely to increase the chances of developing a new anti-mycobacterial drug that targets the cytochrome bcc:aa3 complex.

Therefore, I do not feel that this work is suited for the broad readership of Nature Communications. It would be better suited in a more specialized journal.

**Open Access** This Peer Review File is licensed under a Creative Commons Attribution 4.0 International License, which permits use, sharing, adaptation, distribution and reproduction in any medium or format, as long as you give appropriate credit to the original author(s) and the source, provide a link to the Creative Commons license, and indicate if changes were made.

In cases where reviewers are anonymous, credit should be given to 'Anonymous Referee' and the source.

The images or other third party material in this Peer Review File are included in the article's Creative Commons license, unless indicated otherwise in a credit line to the material. If material is not included in the article's Creative Commons license and your intended use is not permitted by statutory regulation or exceeds the permitted use, you will need to obtain permission directly from the copyright holder.

To view a copy of this license, visit <https://creativecommons.org/licenses/by/4.0/>

## Reviewer #1

1) .... With the advent of cryoEM as structural biology technique, the enzymes and the super complexes of the ETC from Mycobacteria and related bacteria have been determined illuminating their architecture and mode of drug binding providing way for better design of small molecules. Here, the authors purify and determine the structure of the super complex containing bcc and aa3 type oxidase from *M. abscessus* revealing conserved and salient features. Analysis of the binding pocket in one subunit, where the drug binds and that inhibits *M. tuberculosis* reveal differences and this was exploited to design a new drug, which showed high potency against *M. abscessus* and related species. The determined structure with the drug showed the mode of binding, explaining how small changes in the residues (here Glu to Asp and Ala to Leu) can make a huge difference. The major strength of the manuscript is the explanation of the binding mode of inhibitor and mutagenesis to show how the activity is affected.

Thank you for the positive summary of our manuscript and highlighting that the presented study “explains how small changes in the residues (here Glu to Asp and Ala to Leu) can make a huge difference”.

2) An important thing that is not clear to me from the materials and methods, how the water molecules were modelled. The reported resolutions of the two maps are ~2.3 and 2.9 Å but the same number of modelled water molecules (74 – from the PDB validation files) is given for both models. The modelled water molecules are shown in figures 4 and 8, and described in the sections of proton pathways and H<sup>+</sup> translocation. How were they modelled? Were they derived from previous models of other structures? One would expect the map with inhibitor and higher resolution should have more water molecules (in theory at least). Some description of this will be useful and to be added in the method.

Thank you for the feedback. The regions where water molecules were identified had high resolution, as evidenced from supplementary figures 1E and 8D (Apo: 2.5-2.75 Å, Inhibitor-bound: 2.25-2.5 Å), supporting the assignment of water molecules. The water molecules were then modelled based on the 2.8 Å cryo-EM structure of the *Corynebacterium glutamicum* cyt-*bcc:aa3* supercomplex published by Kao, W. C. et al (2022). This is now mentioned in the newly formulated “Model building and refinement” section under Material and Methods, “The water molecules present in the structures were modelled based on the high-resolution cryo-EM structure of the *Corynebacterium glutamicum* cyt-*bcc:aa3* supercomplex (22).”

In addition to the reference model, stabilising hydrogen bonds and strong density signals were used to assign the water molecules with higher confidence. The use of sharp maps in both data sets meant that there is a high signal volume and the stringent assignment of the water molecules based on the conditions mentioned above aims to avoid misassignment of water molecules. The apo model was used to build the inhibitor-bound model and although the number of water molecules in both models are the same, the position of the water molecules has small shifts based on the respective maps.

3) The method section describing the cryoEM imaging data collection and processing is condensed and has not much details (and also not in the supplementary figure describing the workflow). Example, lines 403 and 413 says data processing was performed with cryosparc. Here or in the workflow, how the movies were filtered (criteria for curation), how many models/classes were requested for ab-initio, 3D classification can be described. Also, in the references (34,35) – one for cryosparc and Relion is given (I presume for global refinement). For a casual reader, reference 35 – Zivanov et al indicates that relion was used but this is not

case here but for aberration correction. A reference for non-uniform refinement should also be added (Punjani et al 2020).

Thank you for the feedback. The figure legends for supplementary figures 1C and 8C have been modified as follows, to describe the cryoSPARC data processing workflows in greater detail:

### **Supplementary Figure 1C**

Cryo-EM data processing workflow. The data processing pipeline was performed in cryoSPARC v3.3.1. 6,845 movies were collected and subjected to motion correction (MotionCor2) and CTF estimation (CtFind4). The processed micrographs were subsequently curated with the following thresholds: CTF fit resolution Min: 3.597 Å; Max: 7 Å and Astigmatism Min: 0.47 Å; Max: 500 Å resulting in the acceptance of 5541 exposures for downstream processing. The *M. smegmatis* cyt-*bcc:aa3* oxidase structure (PDB: 6ADQ) was imported into cryoSPARC and used to generate templates for template-based picking yielding 956,580 particles. The particles were binned by a factor of 4 during the particle extraction process to reduce computational time and subjected to multiple rounds of 2D classification. 26 classes containing 334,881 particles were selected to construct an ab initio model with C1 symmetry. The ab initio model accepted 252,300 particles which were then reextracted at full resolution and subjected to non-uniform refinement resulting in a refined map with 249,718 particles with an overall resolution of 3.29 Å. A 3D classification job was performed to classify the particle into 3 classes using C1 symmetry. Class 0 emerged as the largest class with 137,735 particles which was then subjected to local CTF refinement followed by non-uniform refinement. The resulting map, which had an overall resolution of 3.08 Å, was refined further using global CTF refinement and another round of non-uniform refinement yielding a final cryo-EM map with an overall resolution of 3.29 Å with 137,735 particles.

### **Supplementary Figure 8C**

Cryo-EM data processing workflow. The data processing pipeline was performed in cryoSPARC v3.3.1. 6,845 movies were collected and subjected to motion correction (MotionCor2) and CTF estimation (CtFind4). The processed micrographs were subsequently curated with the following thresholds: CTF fit resolution Min: 3.597 Å; Max: 7 Å and Astigmatism Min: 0.47 Å; Max: 500 Å resulting in the acceptance of 5,641 exposures for downstream processing. The *M. smegmatis* cyt-*bcc:aa3* oxidase structure (PDB: 6ADQ) was imported into cryoSPARC and used to generate templates for template-based picking yielding 310,392 particles. The particles were binned by a factor of 4 during the particle extraction process to reduce computational time and subjected to multiple rounds of 2D classification. 19 classes containing 198,256 particles were selected to construct an ab initio model with C1 symmetry. The ab initio model accepted 196,031 particles, which were then reextracted at full resolution and subjected to non-uniform refinement resulting in a refined map with an overall resolution of 2.58 Å. A 3D classification job was performed to classify the particle into 2 classes using C1 symmetry. Class 1 emerged as the largest class with 136,434 particles which was then subjected to non-uniform refinement. The resulting map, which had an overall resolution of 2.51 Å, was refined further using local CTF refinement and another round of non-uniform refinement yielding a final cryo-EM map with an overall resolution of 2.26 Å with 136,434 particles.

In addition, the reference list has also been modified accordingly in the main text:

38. Punjani, A., Zhang, H. & Fleet, D. J. Non-uniform refinement: adaptive regularization improves single-particle cryo-EM reconstruction. *Nature Methods* **17**, 1214-1221, doi:10.1038/s41592-020-00990-8 (2020).

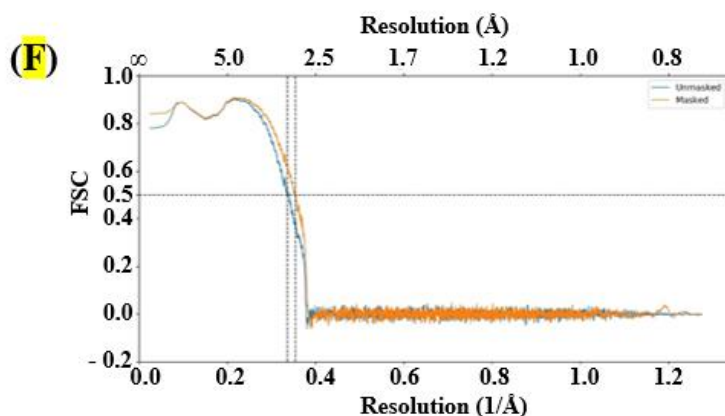
4) Line 403 and 414 says ‘structure refinement was done using COOT and Phenix software’ should rather be ‘Model building and refinement was performed using Coot and Phenix’. This should be expanded (as described in point 1, how was the initial model obtained – denovo or previous PDBs), modelling of ligands etc., If this is included here, then the section heading should read ‘CryoEM data collection, processing, model building and refinement’ instead of ‘CryoEM data collection, processing’. Also, reference number 36 is not apt here and more appropriate references are Emsley et al 2004 (Acta D) and Casanal et al 2020.

This is now mentioned in the newly formulated Model building and refinement section under Material and Methods, “The atomic model of the cytochrome *cyt-bcc:aa<sub>3</sub>* oxidase was built in using the automated protein structure homology-modelling server SWISS-MODEL using the PDB model of the cytochrome *cyt-bcc:aa<sub>3</sub>* oxidase from *M. smegmatis* (6ADQ) as reference structure (3, 41). Thereafter, manual backbone tracing and docking of side chains in the respective map densities was done before performing real-space refinement in Phenix (version 1.20.14487) (40). The refinement results were used to manually inspect and corrected the structures accordingly. The finalized model was validated by the MolProbity online server (42). Map-to-model cross validation was performed in Phenix (version 1.20.14487). FSC<sub>0.5</sub> was used as cutoff to define resolution. The water molecules present in the structures were modelled based on the high-resolution cryo-EM structure of the *Corynebacterium glutamicum* *cyt-bcc:aa<sub>3</sub>* supercomplex (22). ND-011458 was modelled by modifying Q203 from the ligand ID HUU. A summary of the model parameters and the corresponding cryo-EM map statistics is found in Supplementary Table 2B. The finalized model was visualized using ChimeraX (18).”

5) In supplementary figure 1 and 6, the FSC curves showing the map vs model should be included and resolution reported at 0.5.

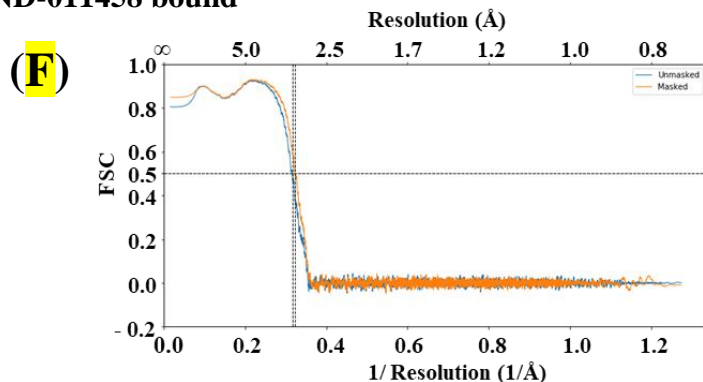
The curves (see below) have been added accordingly for both the Apo (Supplementary Figure 1F) and the ND-011458 bound models (Supplementary Figure 8F).

#### Apo





## ND-011458 bound



6) Figure 1 is not referred in the text and the relevance of having in the manuscript is not clear. I don't think it adds any value. If in case this needs to be retained then best be as a supplementary figure.

Figure 1 is now referred to in the introduction to underscore the evolutionary diversity of the electron transport chain among humans, commensal bacteria and mycobacteria and modified according to reviewer #2 suggestions.

7) Line 93 – is the native PAGE mentioned a ‘blue-native PAGE’? If yes, reference needs to be added and described in the methods.

The native PAGE mentioned is not a ‘blue-native PAGE’.

8) Line 99-100 – 6,845 movies yielded 249,718 particles. This sentence needs rephrasing as the original particles after picking is 956580, but of the 6485, 1305 movies were removed (as per Supp Fig 1).

This has been corrected to “6,845 movies were collected and subsequently curated with the following thresholds: CTF fit resolution Min: 3.597 Å; Max: 7 Å and Astigmatism Min: 0.47 Å; Max: 500 Å resulting in the acceptance of 5,541 exposures for downstream processing. The accepted exposures yielded 249,718 particles that were refined to reach an overall resolution of 3.2 Å (Supplementary Figure 1C-D).” in the manuscript.

9) For supplementary figures 2-4, I have few suggestions. In Supp figure 2, the cartoon representation be replaced with stick representation so that the backbone tracing can be easily followed. In supp figure 3, in my opinion, the interacting/surrounding residues of the ligands within the density should also be shown, in particular for the metal ligands as they look odd by themselves. In supp figure 4, can the backbone be changed to another color instead of gray as the map is also in the same color. In all these figures, the contour level used for the maps be given in the legend and I presume made using Pymol. If yes, then the reference to be added.

The figures have been modified as advised with the contour level mentioned in the respective figure legends. The density map images were made using ChimeraX.

10) In the main figure 3, I feel that it is important to have the cryoEM map as the modelling is based on the map (and the experimental data). So, a panel with the map colored as in 3A will be very helpful. In panel A, density for SOD is shown – how was this figure made i.e., to show only SOD density and it is mentioned (line 121-123) seen at low resolution at 7.5 Å (if it was made with Chimera, then the reference needs to be included). Not clear if it is visible only lower threshold as it is smeared out due to sharpening. In this regard, did the classification or ab-initio give any hint of populations with and without SOD. Can this be

elaborated perhaps in the methods. In panel 3A, can the assembly factor be labelled (PRSAF and LpqE)? Bit difficult to spot them as the colors are similar (but possible when panel B is referred).

The coloured EM map has now been added as advised. In addition, PRSAF and LpqE have also been labelled in Figure 3A. With regards to the SOD, it is visible in some 2D classes leading to the presence of density in the ab initio model as shown in supplementary figure 1B and C. However, given the lack of orientations of the SOD in 2D class, it could not be resolved well in the structure. Despite the low resolution, we wanted to highlight that the SOD is present in the *Mab* cyt-*bcc:aa3* oxidase. In terms of the figure preparation, the density was included by opening the fitted cryo-EM map and model in chimeraX and obtaining the SOD density image at volume level 0.0488 (step 1) and subsequently cropping it out. This is now highlighted in the manuscript, “The density of the SOD was cropped from ChimeraX and added separately to the 2.6 Å cryo-EM map to highlight the presence and association of the dismutase to the *Mab* cyt-*bcc:aa3* oxidase (18).”

11) The sentence in line 123 – ‘The catalytically active CtaC and CtaD contain their cofactors within the cyt-aa3 domain are CtaC and CtaD’ – doesn’t make sense.

Thank you and apologies for the error. This has been corrected to “The catalytically active subunits that contain their cofactors within the cyt-*aa3* domain are CtaC and CtaD.” in the revised manuscript.

12) I am not sure if the section electron and proton translocation pathway needs to be in this detail. I guess these are not new structures i.e., high similarity between the structures of Mab with Msmeg/Mtb and related species. Will it help to focus only on key features.

The current high-resolution structure allows for the complete description of the key pathways in a mycobacterial *cyt-bcc:aa3* for the first time, which has not been possible in previous publications either due to lower resolution or different focus. We believe that the description here can help provide a detailed outlook for readers and in particular medical chemists for the design of novel agents, which can also be extended beyond *M. abscessus* to closely related pathogenic mycobacteria species.

13) Figure 4 is perhaps easily understood by experts in the field of structural bioenergetics but not by a non-expert. For instance, panel A can have surface representation of the protein and highlighting ligands and in the rest of the panels also the cartoon from the protein molecule dominates (make them thinner or change from cylinder to another form).

Thank you for the feedback. Figure 4 has been modified as advised.

14) Line 137, I think the Fig. 3B should be 4B

Thank you and apologies for the error. This has been corrected to, “The distinct coulombic densities for MQH<sub>2</sub>/menaquinone (MQ), at the Q<sub>o</sub> sites and Q<sub>i</sub> sites, (Supplementary Fig. 4), illuminated the bifurcated electron pathway and highlighted the strong interaction with neighbouring residues in the vicinity (Fig. 4B).” in the revised manuscript.

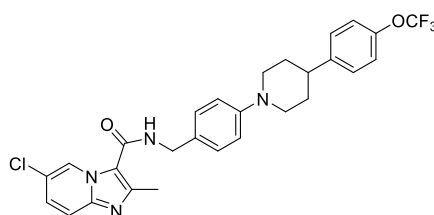
15) In the section, residues responsible for Q203 inactivity .. there is description of residues and the cavity being smaller. But it would help to give some numbers by providing the volume/size of the cavity in different species (example as shown in panel 5B). This would help because in line 218, it is mentioned ‘the reduction in the Mab cyt-*bcc:aa3* cavity volume’.

KV Finder and ChimeraX were utilised independently to identify the inhibitor binding cavity. However, the cavities could not be identified completely by both software preventing the accurate measurement of the cavity volumes.

16) In figure 5, the comparison (panel A) of 3 models has closely related colors – blue (Mtb, apo), green or cyan (Mtb +Q203) and purple (Mab), this makes it difficult to follow, can this be relooked.

Thank you for the feedback. Figure 5A has been modified as advised.

17) In figure 7A, the structure of ND-011458 has a cyclobutane ring in position 1 (a square), is this correct? I thought the compound was synthesized to have only a methyl group from Q203 (I am not a chemist, so I might be wrong in this). In the supplementary figure showing the synthesis (and in validation file), the molecule doesn't have this.



Thank you for the comment. ND-011458 does not contain a cyclobutane ring in position 1 as shown above and is not present in the file here. This is possible due to an error when the structure was added to PowerPoint. The structure has been inserted again to rectify the issue.

18) Line 242, this refers to Fig 6E, should this be 7E?

This has been corrected in the manuscript, “The specificity of ND-011458 for the *Mab* *cyt-bcc:aa3* was determined next with the recombinant *Mab* *cyt-bcc:aa3* oxidase, where ND-011458 reduced respiration levels compared to the vehicle control (Fig. 7E).”

19) In Supplementary figure 6, the panel A is not required (doesn't add much).

Figure 6A has been removed.

20) Figure 8 needs some rethink. It is important to show the density of the ligand (ND-011458) more clearly along with surrounding residues. In the current form, it is shown but not so good. I think panel D should come after panel A and then B/C. In panel B and C, secondary structures can be removed or made thin (like suggested for figure 4). In particular, panel C looks odd with a grey background.

Thank you for the feedback. Figure 8 has been modified as advised.

21) Line 282, as revealed in figure 8A, CFZ reduced the MIC<sub>50</sub>? CFZ is not shown anywhere, should this refer to panel 8E?

This has been corrected in the revised manuscript, “Here, we investigated the interaction of ND-011458 with CFZ. As revealed in figure 8E, CFZ reduced the MIC<sub>50</sub> of ND-011458 in a concentration-dependent manner.”

22) Line 301, ‘Guided by these insights, we discovered ND-011458 ..’ I think more appropriate will be ‘Guided by these insights, we designed ND-011458’. This is because a new drug has not been identified from a library or from scratch but merely restricting to only

a methyl group from an existing compound guided by the structure. In this regard, a MSA of different species of Mycobacteria and other related bacteria focused only on the QcrB or the cavity region might add value.

We wrote now: “Guided by these insights, we designed ND-011458”. In addition, the MSA of different species of Mycobacteria focused on the cavity region has been added as Supplementary Fig. 6 and referred to in the main text (Line 251), “The steric hinderance associated with the ‘blockade’ effect caused by *Mab* QcrB residue L314, which is not present in other pathogenic mycobacterial species (Supplementary Fig. 6), inspired a hit identification attempt where the ethyl group at position 1 in the imidazo[1,2-a]pyridine (IP) core was “shortened” to a -methyl, leading to the generation of the analogue ND-011458 (Fig. 7A; see Supplementary Information: *General synthesis routes to compounds*).

			*	*	
<i>M. tuberculosis</i>	313	T	E	G	L A R 318
<i>M. smegmatis</i>	308	T	D	G	L I R 313
<i>M. abscessus subsp abscessus</i>	310	T	D	G	L L R 315
<i>M. abscessus subsp bolletii</i>	293	T	D	G	L L R 298
<i>M. abscessus subsp massiliense</i>	302	T	D	G	L L R 307
<i>M. avium</i>	323	T	E	G	L A R 328
<i>M. marinum</i>	323	T	E	G	L A R 328
<i>M. fortuitum</i>	308	T	E	G	L A R 313
<i>M. peregrinum</i>	308	T	E	G	L A R 313
<i>M. kansasii</i>	313	T	E	G	L A R 318
<i>M. intracellulare</i>	308	T	E	G	L A R 313
<i>M. chelonae</i>	318	T	E	G	L A R 323
<i>M. leprae</i>	312	T	E	G	L A R 317

**Supplementary Figure 6.** QcrB cavity region sequence alignment between mycobacterial species

23) In table 2B, the particle images/numbers need to be revised. When it says selected, it can be from any of the steps from picking to classification. May be an easy way is to use the initial particle numbers – after autopick and then clean up after 2D classification (before ab-initio) and then final number contributing to the map. Here, in the ND-011458 data, the numbers are different than in the work flow (supp figure 6), please check. The applied B-factor (Å<sup>2</sup>) should be with negative sign (as the map is sharpened). Global resolution is mentioned as 2.66 but the validation file has 2.85 Å. Tables 2A and 2B can be combined by removing the whole image processing section as this is mentioned in the methods.

Tables 2A and 2B have now been combined as advised and the particle numbers have also been revised accordingly. The global resolution of the inhibitor free map is 2.66 Å as evidenced by the GFSC curve. During the PDB validation process, the initial map submitted was 2.85 Å while the revised map submitted is 2.66 Å. However, the PDB team did not update the resolution on PDB validation report.

24) In table 2C, the number of residues is the same for both the models. This is surprising as one of them has ligand (2 numbers). In the validation file, I notice that chain k/l in the apo model has 144 residues (46750 atoms as in the validation file) and, in the inhibitor, bound structure has 145 residues (46789 atoms in the validation file). Summing up the number of residues in the validation file gives a number of 5756 for the dimer, which is different from 5634 in the table. Please check. I would recommend the table to be expanded to include number of residues for proteins, ligands, water separately and the B-factors (after model

refinement) for each of them. Alternatively, number of atoms (for proteins, ligands and water) can be mentioned instead of residues as done routinely in crystallographic structures.

Thank you for the feedback and apologies for the confusion. The number of residues for proteins, ligands and water are now indicated separately. The applied B-factor ( $\text{\AA}^2$ ) is mentioned in Table 2A.

25) In the PDB validation file of the apo structure (9WCX), there is one peculiar bond length outlier (among others) – chain X, Thr43, the N-CA is 2.52  $\text{\AA}$ , which is 1.1  $\text{\AA}$  longer than the ideal values. Please check this.

Thank you for pointing out the mistake. The distance is now corrected to 1.50  $\text{\AA}$ .

26) Line 237 – IC50, change 50 to subscript

This has been corrected in the manuscript.

27) Line 367 – should be ‘100  $\mu\text{g/ml}$  3x FLAG peptide’

This has been changed to, “The protein was eluted with buffer D (20 mM MOPS [pH 7.4], 100 mM NaCl, 2 mM Pefabloc, 1 mM PMSF, 0.01% [vol/wt] DDM, 100  $\mu\text{g/ml}$  3xFLAG)”.

28) Line 397 – I think this should K3 and not K2. If it is K2, then the exposure time has to be higher (not 2.83 s as mentioned in line 400).

We wrote: “Images were taken using an FEI Titan Krios electron microscope operating at 300 kV with a K3 Summit detector (Gatan, Pleasanton, CA) at a magnification of  $\times 130,000$ .”

29) Line 401/412 – it should be CTF estimation and not refinement. CTFFIND4 estimates the CTF from the images.

This has been changed to, “Motion correction was performed using MotionCor2 and CTF estimation was performed using CTFFind4 (32, 33).”

30) Line 410 – 0.5 to 1.5  $\mu\text{m}$  and not  $\mu\text{M}$

We corrected this as follows: “A defocus range of 0.5 to 1.5  $\mu\text{m}$  was implemented. Movies were collected at 40 frames per stack with an exposure time of 2.83 s.”

31) Line 460 – should read, ‘In this assay, Laminin/poly-D-lysine ...’

We wrote now: “In this assay, Laminin/Poly-D-lysine was used as cell adhesive to attach the cells onto the plate.”

32) Figure 2 panel A, there are 3 lanes labelled as -, + and Mab, two showing positive signal in Western blot. Are these two lanes with different concentration or volume? Or in other words, what are (+), Mabs. The lane numbers can be given in the bottom.

We apologise for the confusion. The symbols reflect the following: (-) *Mabs* WT serving as negative control, (+) *Mtb* *cyt-bcc:aa3* oxidase with FLAG/6 $\times$ HIS tag serving as positive control, (*Mabs*) *Mabs* strain with Genomic FLAG/6 $\times$ HIS tag. The figure legend has been modified in the manuscript for better clarity as advised, “Western blot analysis confirms expression of QcrB C-terminal genomic FLAG tag in recombinant *Mab* strain derived from ORBIT-promoted gene alteration (Lane 4) with positive (+, *Mtb* *cyt-bcc:aa3* with QcrB C-terminal FLAG tag, Lane 3) and negative (-, *Mab* WT, Lane 2) controls.”

33) Figure 7, panel A, Design of Q203 analogues with modifications at position 1. Were there many more analogues made?

This has been corrected to “Design of Q203 analog with modification at position 1.” in the manuscript.

## Reviewer #2

1) Of four mutational differences near the active site, they determined by site-directed mutagenesis that two were important, and designed a new inhibitor based on the structure that should be more effective against *M. abscessus*. They prepared a tagged strain of the complex, purified it, and solved the structure of the native complex, one with menaquinone in the binding sites and the other with the new inhibitor in the Q<sub>o</sub> site. The work is sound and significant, ....

We are glad, that reviewer #2 describes the manuscript as being “sound and significant”.

2) Fig 1. On the left hand figure, showing the mitochondrial situation, the space below the membrane is labeled cytoplasm. This is OK if we ignore the outer mitochondrial membrane due to its permeability. But the space above should then be "mitochondrial matrix", not periplasm. To further confuse, the membrane is concave downward, suggesting that the cytoplasm is inside and the matrix or periplasm is outside.

On the other hand if we assume the labeling is for bacterial counterparts, with cytoplasm = matrix below and periplasm = inter-membrane space above, the orientation of the complexes is wrong, as cyt *c* and the P-side of the complexes should be in the inter-membrane/periplasmic space.

Thank you for the feedback and apologies for the confusion. The figure has been amended as advised.

3) Fig 1 legend, line 549: ". . the dominant oxidase cyt-bo<sub>3</sub> (cyan-green) resembles a CIII-CIV like assembly" insert the word "functionally", because structurally there is little similarity.

Thank you for the valuable suggestion. This has been amended in the manuscript, “Commensal bacteria like *Escherichia coli* (*E. coli*), which colonize the gut, have a branched respiratory pathway where the dominant oxidase cyt-bo<sub>3</sub> (cyan-green) resembles a CIII-CIV like assembly functionally.”

4) 114-116: The description of subunit qcrC seems to be wrong- the trans-membrane helix is on the C-terminal end, not the N-term as implied here. That is, "after" the periplasmic heme-binding domain, not before.

This has been corrected to “QcrC consists of a periplasmatic domain with two heme-containing cytochrome *c* domains, referred to as cyt-*c*<sub>I</sub> and cyt-*c*<sub>II</sub>, followed by a single transmembrane-spanning  $\alpha$ -helix (Fig. 3B).”

5) lines 142-144, 304: "low-spin, high-spin, heme". Is this supposed to be low, high potential heme? Both B hemes are low spin, with bi-axial histidine coordination.

We wrote now: “The second electron from the semiquinone is transferred to the low potential heme *b*<sub>L</sub> located 19 Å away (Fig. 4C). The electron from heme *b*<sub>L</sub> is transferred via L222 to the high potential heme *b*<sub>H</sub> (14 Å distance), to a bound MQ at the Q<sub>i</sub> site to allow for the generation of MQH<sub>2</sub> and establishment of the Q-cycle (Fig. 4C).”

6) 94 ". . . the presence of hemes a, b and c," -There is a convention, (although maybe not official), of referring to heme with capital letters when just specifying the type of heme, i.e. the substance, rather than heme of a specific cytochrome. thus, "heme *b*<sub>L</sub> and heme *b*<sub>H</sub> are both B hemes, the complex contains two heme B molecules". I leave up to the authors' discretion.



The nomenclature chosen follows the initial publications that described the *M. smegmatis* *cyt-bcc:aa3* (Gong et al, 2018 and Wiseman et al, 2018). Since the publications were the first to describe a mycobacterial *cyt-bcc:aa3*, the nomenclature was retained to help the readers have better ease when reading related articles.

7) line 315- protonatable QcrB residue s155 D311, R315, D304 and E272, E272 is in qcrC, according to figure 4. This should also be made clear here.

This has been amended: “The first proton exit pathway is aligned with protonatable QcrB amino acids D311, R315, D304 and QcrC residue E272, located in the vicinity of a water channel and allowing proton translocation via a Grotthuss transport mechanism (23) and an QcrA and QcrB interface to the periplasmic region (Fig. 4D).”

8) The oxygen consumption assay in Figure 2E is problematic and needs more explanation. It should be stated what is added at ~50 s. If I understand correctly, the enzyme was present from the start and reduced DMNQ was added at 50 s. The decrease in oxygen in the control could be due to dilution by the anaerobic DNQH<sub>2</sub> solution, but only if the dilution is greater than 2-fold (volume of DNQH<sub>2</sub> is not given). Otherwise there is concern that the reduction is due to residual BH<sub>4</sub>, H<sub>2</sub> reacting at the platinum Clark electrode, or some rapidly auto-oxidizable substance reduced by BH<sub>4</sub>. In the trace with enzyme, the decrease in O<sub>2</sub> on adding DMNQH<sub>2</sub> is greater, reaching nearly to zero, mostly within about 10 sec. The assumption would be that this is due to oxygen consumption by the complex. Using a lower concentration of enzyme might permit to resolve the enzyme activity from the dilution effect and electrode kinetics. Or maybe I completely misunderstand the assay, due to lack of description. It would be nice to have a third trace with enzyme plus inhibitor, and a fourth trace with enzyme + KCN or other inhibitor of the oxidase (is NQH<sub>2</sub> reacting at Qo, or directly with the C hemes?). Finally, adding dithionite at the end would establish the zero O<sub>2</sub> level. However, it is understood that the main focus of the paper is on structure not activity, so just providing a better explanation would be acceptable.

Thank you for the feedback. The method section has been modified as follows to provide more detail: “20 mM DMNQ (Enamine, Cincinnati, OH) was prepared in 1 mL of ethanol containing 6 mM HCl. The DMNQ solution was reduced with a few grains of sodium borohydride (NaBH<sub>4</sub>) in an ice bath. Then, 10 µL of 12 N HCl was used to quench the reaction. This reaction resulted in the formation of DMNQH<sub>2</sub>. A serial 2-fold dilution of the 20 mM DMNQH<sub>2</sub> solution, in absolute ethanol, was performed till a 2.5 mM solution of DMNQH<sub>2</sub> was obtained to minimize the presence of NaBH<sub>4</sub> in the final solution. The oxygen consumption assay was performed based on published protocols (3-5). Briefly, a 1mg/ml stock of the purified *Mab* *cyt-bcc:aa3* oxidase was resuspended in 500 µL of reaction buffer (20 mM MOPS [pH 7.4], 100 mM NaCl, 0.01% DDM) to a final concentration of 65 nM and added into the reaction chamber. The baseline was monitored using a Clark-type oxygen electrode (Oxytherm+, Hansatech, Pentney, United Kingdom) for 50 s. 5 µL of 2.5 mM DMNQH<sub>2</sub> was then injected into the reaction chamber to achieve a final DMNQH<sub>2</sub> concentration of 25 µM and initiate respiration within the oxidase. The reaction chamber was immediately sealed, and oxygen consumption was monitored till a plateau was achieved. The oxygen consumption curves were plotted using GraphPad Prime 8.0 software (34).”

9) Line 135: "The distinct coulombic densities for MQH<sub>2</sub> and menaquinone (MQ), at the Qo sites and Qi sites, respectively . . ." Can you really distinguish MQ from MQH<sub>2</sub> at this resolution)? And, if the enzyme is active it should oxidize MQH<sub>2</sub> at Qo and reduce MQ at Qi, giving the opposite of what you suggest. More likely both would be oxidized when applied to the grid, maybe reduced by the electron beam/radiation damage.



The current resolution does not allow for the distinction between MQ and MQH<sub>2</sub>. The section has been reformulated for better clarity as follows: “The distinct coulombic densities for MQH<sub>2</sub>/ menaquinone (MQ), at the Q<sub>o</sub> sites and Q<sub>i</sub> sites, (Supplementary Fig. 4), illuminated the bifurcated electron pathway and highlighted the strong interaction with neighbouring residues in the vicinity (Fig. 4B). The current resolution does not allow for the clear distinction between MQH<sub>2</sub> and MQ thus requiring the need to rely on the spatial arrangement at the active sites to predict the most likely candidate observed. Under physiological conditions, efficient transfer of electrons is hindered when the distance extends beyond 14 Å (19). In the Q<sub>o</sub> site, the edge-to-edge distance from the electron carrier to heme *b*<sub>L</sub> is 19 Å which exceeds the 14 Å limit for efficient physiological electron transfer. Furthermore, recent cryo-EM studies found Q203 to bind deeper within the Q<sub>o</sub> site, suggesting that the endogenous electron donor MKH<sub>2</sub> occupies a deeper position within the pocket for efficient electron transfer (20, 21). This suggests that the density observed in the Q<sub>o</sub> site would most likely correspond to an oxidized product leaving the active site. On the other hand, the density for the electron carrier at the Q<sub>N</sub> site, is 9 Å away from heme *b*<sub>H</sub> allowing for efficient electron transfer. This implies that the density observed in the Q<sub>N</sub> site would most likely correspond to either MQ or partially reduced semi-MQ.”

10) line 239 and 623- "ND-011458 was able to achieve the characteristic respiratory burst observed for Q203 in *Mtb*". Need to briefly explain why a respiratory inhibitor causes a respiratory burst. Is respiration going by an alternate oxidase with lower efficiency, thus needing more O<sub>2</sub>?

Lamprecht et al showed that the increase in OCR, in the presence of Q203, is due to the electron flux being rerouted to cytochrome *bd* oxidase, which consumes O<sub>2</sub> at a higher rate. This explanation is now added in the manuscript for both instances: “The effect of the analogue on whole cell respiration in *Mab subsp. abscessus* mirrored a profile of Q203 in *Mtb* (Fig. 7D), where an increase in oxygen consumption rate (OCR) is observed upon the addition of the inhibitor (25). This phenomenon is attributed to the electron flux being rerouted to cytochrome *bd* oxidase which consumes oxygen at a higher rate (25).” and “ND-011458 was able to achieve the characteristic respiratory burst observed for Q203 in *Mtb* due to the electron flux being rerouted to cytochrome *bd* oxidase which consumes oxygen at a higher rate compared to the baseline.”

11) line 374, 376. "The oxidized UV spectra" - The shortest wavelength shown is 425 nm.

The spectrum was recorded from 400 to 700 nm to ensure that signals are not missed. We then presented the spectrum starting at the point where the first peak was identified which happens to be 425 nm.

12) I did not have access to the structure coordinates files, which are on hold until publication. I would have liked to see if they found the cis-prolines at residues 138, 257, and maybe 421 in *qcrB*. The validation reports from Protein Data Bank were made available, and did not raise any alarms. But then I am not very familiar with cryo-EM methods and validation.

Thank you for the comments. The structure has been validated by PDB, and the requested modifications have been made and accepted by PDB. The residues 138, 257, and 421 are all trans-prolines.

13) The resolution is given as 2.6 Å. Which of the two structures is this for? Do they both have the same resolution?

The inhibitor-free structure has a resolution of 2.66 Å while the ND011458-bound structure has a resolution of 2.26 Å as reflected in Supp. Table 2B.

14) Sup fig 1 legend: (B) "2D- classification in of picked particles in . . ." delete "in" or "of"

This has been corrected to “2D-classification of picked particles in CryoSPARC.” in the figure legend.

### Reviewer #3

#### 1.) Overall, the manuscript is well-written, and the figures are clear.

We are glad, that reviewer #3 finds the manuscript being well-written, and that the figures are clear.

2) However, I have concerns about the novelty of the work. Currently, there are 15 mycobacterial cytochrome bcc:aa3 structures available in the protein data bank and 7 papers that describe these. There are no major differences between the new *M. abscessus* structure and previous structures that change the interpretation of catalytic cycle. Hence, the detailed description of this cycle presented on pages 5-8 (lines 105-182) is a repeat of earlier work (see doi: 10.1038/s41594-018-0160-3, 10.1126/science.aat8923, and 10.1038/s41467-024-49628-9.)

The structures of the *Mab* cyt-bcc:aa3 oxidase in the absence and presence of an inhibitor at 2.6 Å and 2.3 Å resolution, respectively, are the first high resolution structures of an entire mycobacterial cytochrome oxidase supercomplex (the structure 7E1W is an engineered hybrid of an *Mtb* cyt-bcc and an *M. smegmatis* cyt-aa3 oxidase) of a mycobacterial pathogen. Such resolution enabled for the first time the assignment of water molecules, essential for proton translocation to the intermembrane space to contribute to the proton motive force as well as to the catalytic center, to enable oxygen reduction to water. As reflected by the table below, no water molecule could be assigned to any proton channel within the structures before. These processes are fundamental in bioenergetics as well as for the design of novel potent inhibitors.

Strain	<i>M. smeg</i>	<i>M. smeg</i>	<i>Mtb</i>	<i>Mtb</i> / <i>M. smeg</i> Hybrid	<i>M. smeg</i>
PDB ID	6ADQ	6HWH	8HCR	7E1W	7RH7
Resolution (Å)	3.5	3.3	4.5	2.67	3
Water molecules in structure	No	No	No	1 water molecule coordinated with Q203	No

3) The observation that the modification of two residues in the inhibitor binding site or the deletion of one methyl group in the Q203 inhibitor restores sensitivity of *M. abscessus* to this class of compounds is nice, but not surprising.

We respectfully ask the reviewer to think differently for a moment and try to acknowledge:

1. This is the **first** reported structure of cyt-bcc:aa3 in *Mycobacterium abscessus*, a serious health threat with no approved treatments.
2. This is the **first** report of having the natural substrate (menaquinol) bound in a *Mycobacterium abscessus* cyt-bcc:aa3 active site.
3. This is the **first** report of a clinical candidate Q203 (also known as Telacebec) bound in the *Mycobacterium abscessus* cyt-bcc:aa3 active site and a structural basis to why it is inactive.
4. This is the **first** report of a potent analog bound in the *Mycobacterium abscessus* cyt-bcc:aa3 active site and the structural basis as to why it is active.

While not noted in the text, these authors have spent years trying to identify QcrB inhibitors that can potently inhibit *M. abscessus* cyt-bcc:aa3 but were met with little success. The literature even has inaccurate reports of QcrB agents that are active against *M. abscessus*. For instance, the QcrB inhibitor TB47 is **\*not\*** active against *M. abscessus* (see erroneous publication, “Assessment of Clofazimine and TB47 Combination Activity against *Mycobacterium abscessus* Using a Bioluminescent Approach. Antimicrob Agents

Chemother. 2020 Feb 21;64(3):e01881-19. doi: 10.1128/AAC.01881-19;” and our lab’s rebuttal demonstrating that the potency observed was due to the companion drugs (see, “The QcrB Inhibitors TB47 and Telacebec Do Not Potentiate the Activity of Clofazimine in *Mycobacterium abscessus*. Antimicrob Agents Chemother 65:10.1128/aac.00964-21. <https://doi.org/10.1128/aac.00964-21>”). As such, this manuscript definitively explains, why TB47 is not active.

Finding an active compound is not as obvious as the reviewer suggests. For instance, if it is not surprising that deletion of one methyl group (ethyl à methyl) leads to a potent compound what would the reviewer expect the potency of even smaller analog (that is ethyl à H) would be? It would fit very well in the pocket but it was inactive! [Data not included because while the MICs have been confirmed but getting the co-crystal structure has not been successful.] Now, what about the trifluoromethyl analog (that is, CH<sub>3</sub> -à CF<sub>3</sub>)? Perhaps, same potency. Well, it was inactive! [Again, data not shown but the MICs have been confirmed but getting the co-crystal structure has not been successful.] This is an extremely **novel** pocket, and we have just begun to explore the SAR, which we hope to do and publish in due course.

Case in point, we had published on the genetic differences via sequence alignments between various mycobacteria *cyt-bcc:aa3* but that genetic information had enable us to prepare active inhibitors of *Mycobacterium abscessus cyt-bcc:aa3* until we had resolved the crystal structure, rendering this finding very novel and impactful.

4) In addition, the observation that this class of compounds synergizes with clofazimine is not new either, as this has been described before (see doi: 10.1128/aac.00318-25, 10.1016/j.biopha.2020.110782, 10.1128/AAC.01418-21, 10.1128/aac.00318-25, 10.1038/ncomms12393)

Our labs refuted the finding of the first reference (doi: 10.1128/aac.00318-25), in the manuscript, “The QcrB Inhibitors TB47 and Telacebec Do Not Potentiate the Activity of Clofazimine in *Mycobacterium abscessus*. Antimicrob Agents Chemother 65:10.1128/aac.00964-21. <https://doi.org/10.1128/aac.00964-21>.” The TB47 authors did not conduct their experiments properly and did not show synergy with clofazimine. Furthermore, the **novelty** and impact of this work is the structural explanation of why TB47 would not be active against the *Mycobacterium abscessus cytochrome bcc:aa3*. While the data is not shown, we did evaluate TB47 and confirmed it to be inactive, we have not attempted to co-crystallize it to further prove *in vitro* assessment as it was moot point.

The second reference (10.1016/j.biopha.2020.110782) deals with TB47 and clofazimine in *M. tuberculosis* murine infection model and since TB47 is very active against *Mtb* (nanomolar potency) synergy is expected. However, TB47 is **not active** against *M. abscessus*, refuted by our earlier work and the structural reasons can clearly be seen in this manuscript.

The third reference (10.1128/AAC.01418-21) is an error as it **does not mention any synergy with clofazimine**. In fact, it is a repeat and further validation of our own report that Q203 has efficacy in *Buruli Ulcer* published (which was first in Nature Communication 18;9:5370. doi: [10.1038/s41467-018-07804-8](https://doi.org/10.1038/s41467-018-07804-8)). We had even shown that Q203 is highly active, bactericidal, against *Buruli Ulcer* because this unique mycobacterium is lacking *cyt-bd*. As

such, a companion drug is not required. However, Q203 is not active against *M. abscessus* as definitely shown by this manuscript.

The fourth reference (10.1128/aac.00318-25), is TB47 potency in *Mycobacterium leprae*. TB47 (like the previous report on Q203) is very active as a single agent against *M. leprae*, however against *M. abscessus* it is inactive. Therefore, this compound has bactericidal potency by itself because *M. leprae* lacks *cyt-bd* and addition of clofazimine helps to sterilize even faster. However, Q203 is not active against *M. abscessus* as definitely shown by this manuscript.

The fifth reference (10.1038/ncomms12393) explains some of the mechanistic reasons why one would expect synergy between a QcrB inhibitor (Q203) and clofazimine. However, Q203 is not active against *M. abscessus* and this this manuscript explains as to why.

We credit the reviewer by noting that combination of a QcrB inhibitor and clofazimine often leads to synergy but this has never been **correctly** demonstrated in *M. abscessus*. Our results are certainly impactful because QcrB inhibition of *M. abscessus* is still only bacteriostatic and not cidal as in Buruli ulcer or *M. leprae*. In revision of this manuscript, the combination of QcrB and clofazimine is actually not synergist but additive. This challenges up, in our future work, to find a combination which will be sterilizing regime (*in vivo*) as well as exploring the role of *cyt-bd* in *M. abscessus*. These experiments are beyond the scope of this manuscript, which is focused on this novel discovery.

Hindsight is 20/20 and if not for the resolved structure presented in this manuscript it would not be obvious why compounds like TB47 and Q203 do not inhibit *M. abscessus*; otherwise there would be many known QcrB inhibitors of *M. abscessus*. [But to date none are more active than the compound presented herein.]

5) Finally, there are more than twenty Q203-like compounds that have been described to date. Currently, the most advanced of these, Q203, appears to be stalled after the Phase-2 clinical trials. None of the other Q203-like inhibitors has entered the clinical trial stage. This shows that the progress from an initial inhibitor such as ND-011458 to late-stage lead compound such as Q203 is extremely challenging. Thus, the addition of another compound to the growing list of cytochrome bcc:aa3 inhibitors is unlikely to increase the chances of developing a new anti-mycobacterial drug that targets the cytochrome bcc:aa3 complex.

We would like to remind the reviewer of the incredible cost associated to progress a compound through clinical development and advancement of TB drug has a low return on investment. Therefore, we believe that Q203 is stalled not because of poor clinical efficacy but rather because of the funding to run additional clinical trials has to be secured by Qurient. In fact, Q203 was sub-licensed to the TB Alliance in a likely effort to share costs of clinical development. There are few pharma companies or venture capital firms willing to invest the needed \$10-20 million USD to advance a compound for just a TB indication such as sought by Q203.

However, a compound that can target a serious health treat such as *M. abscessus* wherein there are no approved treatments and a much larger potential for profits is more likely to receive financial investment for compound advancement.

The point is that there is a lot of clinical potential and positive impact a QcrB inhibitor can have on human health, but challenge lies in securing the proper investment as mycobacterial

diseases are not seen as highly profitable. However, compounds that target *Mycobacterium avium* complex (MAC) or MABI disease have much bigger markets as there are no approved treatments.

While the authors cannot disclose much, there is a new QcrB inhibitor seeking an IND for treatment of MAC infections. The major set back is in securing ~\$10 million USD for Phase-I clinical trials but already >8 kilograms of GMI compound has been prepared and pills are being pressed for the study. Therefore, advancement of QcrB agents is not at all stalled rather they are emerging but only as fast as funding allows.

This manuscript is very impactful for the field in showing that QcrB is a viable target in *M. abscessus* and drug like compounds can inhibit it.

6) Therefore, I do not feel that this work is suited for the broad readership of *Nature Communications*. It would be better suited in a more specialized journal.

As pointed out above, this manuscript presents a multi-disciplinary approach, resulting in novel outcomes relevant to bioenergetics, microbiology, structural biology, anti-microbial resistance, respiratory diseases caused by mycobacteria, drug target and -discovery as well as medical chemistry. Therefore, this impactful manuscript is very well suited for the broad readership of *Nature Communications*.

Hoping that the completions, and corrections we have made, will make this revised version suitable for publication in *Nature Communications*.

With many thanks for your efforts in advance.